

The effects of turbulence on a separated and reattaching flow

By YASUHARU NAKAMURA AND SHIGEHIRA OZONO

Research Institute for Applied Mechanics, Kyushu University, Kasuga 816, Japan

(Received 28 April 1986 and in revised form 6 October 1986)

The effect of free-stream turbulence on the mean pressure distribution along the separation bubble formed on a flat plate with rectangular leading-edge geometry is investigated experimentally in a wind tunnel using turbulence-producing grids. Emphasis is placed on finding the effect of turbulence scale. The ratio of turbulence scale to plate thickness investigated was about 0.5 to 24 for two values of turbulence intensity of about 7 and 11%. The Reynolds number based on plate thickness was approximately $(1.4\text{--}4.2) \times 10^4$.

It is found that the main effect of free-stream turbulence is to shorten the separation bubble. It is progressively shortened with increasing turbulence intensity. The mean pressure distribution along the shortened separation bubble is insensitive to changing turbulence scale up to a scale ratio of about 2. With further increase in the scale ratio it asymptotes towards the smooth-flow distribution. There is no trace of interaction between turbulence and vortex shedding (the impinging-shear-layer instability) in the mean pressure distribution.

1. Introduction

The flow in the Earth's boundary layer is highly turbulent, and this can significantly influence the wind loads experienced by buildings and structures. The effect of free-stream turbulence on bluff-body mean flow is therefore one of the most important problems in wind engineering. However, the problem has long been a puzzling one (see, for example, Bearman & Morel 1983) because many experiments done to date showed that there is very little or no effect of changing turbulence scale, despite a significant effect of changing turbulence intensity.

We have been concerned with this enigma for several years and found, in a series of wind-tunnel experiments on square prisms and rectangular cylinders (Nakamura & Ohya 1983, 1984, 1986), that bluff-body mean flow is indeed sensitive to changing turbulence scale. It has thus been found that turbulence can selectively control bluff-body mean flow at two main scales. Turbulence of small scale, i.e. a scale comparable with the thickness of the shear layer, can increase the growth rate of the shear layer through enhanced mixing, thereby causing the shear layer to reattach earlier to the side of a bluff body. On the other hand, turbulence of large scale, i.e. a scale comparable with the body size, can strongly interact with vortex shedding from a bluff body. Namely, large-scale turbulence weakens vortex shedding from a two-dimensional bluff body by reducing spanwise correlation while it strengthens vortex shedding from a three-dimensional bluff body through resonant interaction. The mean flow can respond strongly to large-scale turbulence through changes in vortex shedding.

The work described here is concerned with the effects of free-stream turbulence on the mean flow past a two-dimensional flat plate with rectangular cross-section where the separation bubble is generated at the sharp leading edge. As in the previous papers, attention is focused on the special effects of turbulence scale. There have been very few investigations on the effects of free-stream turbulence on separated and reattaching flows. These include Hillier (1976), Bearman (1978), Hillier & Cherry (1981) and Kiya, Sasaki & Arie (1984). All of these investigations reported that the length of the separation bubble was reduced considerably with increasing turbulence intensity but there was no significant effect of changing turbulence scale. For example, Hillier & Cherry showed that the bubble length was insensitive to turbulence scale up to $L_x/h = 1.97$, where L_x is the integral scale of the u -component velocity of turbulence and h is the thickness of the plate, although they found significant effects on fluctuating surface pressures.

In the present paper we explore the effects of turbulence scale over a range much wider than in Hillier & Cherry (1981). Measurements of the mean pressure distributions along the separation bubble were made in a wind tunnel for a turbulence scale of about $L_x/h = 0.5-24$ for two values of turbulence intensity u'/U of about 7 and 11%, where u' and U are respectively the r.m.s. and mean values of the u -component velocity of turbulence.

2. Experimental arrangements and procedures

2.1. Wind tunnel and turbulence-producing grids

The experiments were conducted in a low-speed wind tunnel with a 4 m high by 2 m wide by 6 m long rectangular working section. The tunnel can provide a very uniform smooth flow with a turbulence intensity of about 0.12%. To create a nearly homogeneous isotropic turbulence field, three square-mesh biplanar grids of rectangular-section bars with different mesh sizes were used. The characteristics of the grid turbulence relevant to the present experiment are given in table 1, which lists the mesh size M and the bar size b of the grid, the distance X between the grid and the leading edge of the model, and the intensity and integral scale of turbulence at the leading edge of the model. The 6 m long working section was too short for the experiment using the largest grid (grid C), so the diffuser was modified to extend the length of the working section by 6 m.

2.2. Flat-plate models and measurement procedures

Figure 1 shows the model for a two-dimensional flat plate with rectangular cross-section, which had a thickness ranging from $h = 1$ cm to 6 cm and a chord of 102 cm in length. As is shown in figure 1, end plates giving an effective span of 170 cm were always employed. The model was fitted with pressure taps of 0.5 mm inner diameter on the top and bottom surfaces. The position of the pressure tap is indicated by the distance x measured from the leading edge. Measurements of mean static pressures along the separation bubble were made in the present experiment. The pressure was determined using a calibrated inductance-type pressure transducer, and the mean pressure p is presented in the form of a pressure coefficient $C_p = (p - p_0)/(\frac{1}{2}\rho U^2)$, where ρ and p_0 are respectively the air density and the mean static pressure of the free stream. The model spanned horizontally the 2 m width of the working section at zero incidence with a minimum residual asymmetry top-to-bottom which was of order of 0.03 in C_p . The measurements were made on both surfaces and averages of the top and bottom pressure coefficients are shown in the subsequent figures.

	M (cm)	b (cm)	X/M	u'/U (%)	L_x (cm)
Grid A	13.0	2.5	6	12.8	3.0
			11	6.6	3.9
Grid B	26.0	7.5	8	11.2	8.4
			14	7.3	12.6
Grid C	60.0	15.0	8	11.0	16.5
			14	6.9	24.0

TABLE 1. The characteristics of the grid turbulence

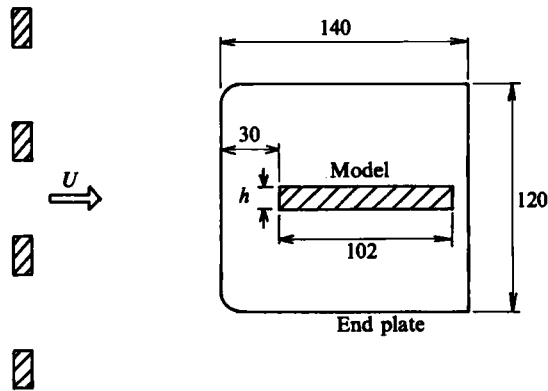


FIGURE 1. Flat-plate model mounted downstream of a turbulence-producing grid. Dimensions in cm.

The main purpose of this investigation was to examine possible effects of turbulence scale on the mean pressure distribution along the separation bubble. This was done by working with six sizes of models, $h = 1, 1.5, 2, 3, 4$ and 6 cm, using three grids with different mesh sizes. The measurements corresponded to two values of turbulence intensity of about 7 and 11% (see table 1). The ratio of turbulence scale to plate thickness ranged from about 0.5–24. The measurements were made at a flow speed of 20 m s^{-1} for models with $h = 1$ and 1.5 cm and of 10 m s^{-1} for the other models. Correspondingly, the range of the Reynolds number in terms of h was about $(1.4\text{--}4.2) \times 10^4$.

In order to gain a better understanding of the interaction between large-scale turbulence and vortex shedding, an experiment was added where measurements of fluctuating flow velocities and mean pressure distributions were made on a flat-plate model with an oscillating leading-edge spoiler in smooth flow. The model was 20 cm in thickness and 3 m in length, and had a $20 \text{ cm} \times 1 \text{ cm}$ leading-edge spoiler. In the experiment the leading-edge spoiler was forced to oscillate, using a Scotch-yoke mechanism, in a lateral direction at a constant frequency of 2 or 4 Hz at an amplitude of 5 or 10% of the plate thickness. The spoiler was initially flush with the flat-plate model to make pressure measurements, and then an upward sinusoidal oscillation was given to make further measurements. It was assumed that the resulting flow changes on the top and bottom surfaces were practically independent, and measurements were made only on the top surface. The range of flow speed was $3\text{--}10 \text{ m s}^{-1}$ approximately. The reduced speed, defined by $\bar{U} = U/(f_y h)$, where f_y is the frequency of spoiler oscillation, ranged from 4 to 25 approximately which included the resonance

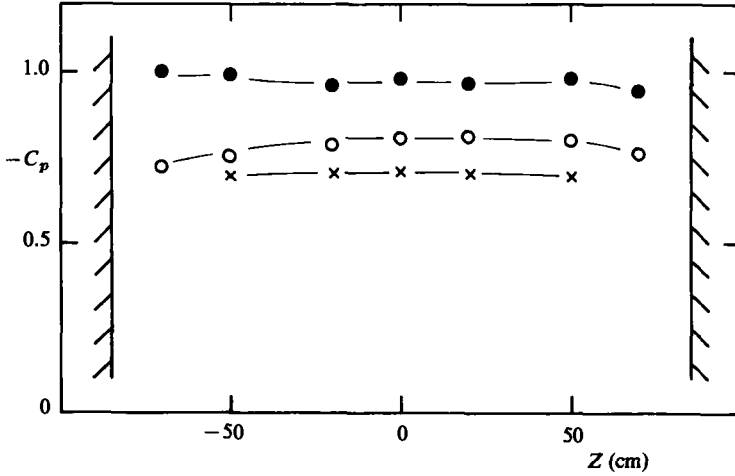


FIGURE 2. Spanwise variation of the pressure coefficient for model with $h = 4$ cm at $x/h = 1$ in smooth and turbulent flows. \times , smooth flow; \bullet , $L_x/h = 1.0$, $u'/U = 6.6\%$; \circ , 6.0, 6.9%.

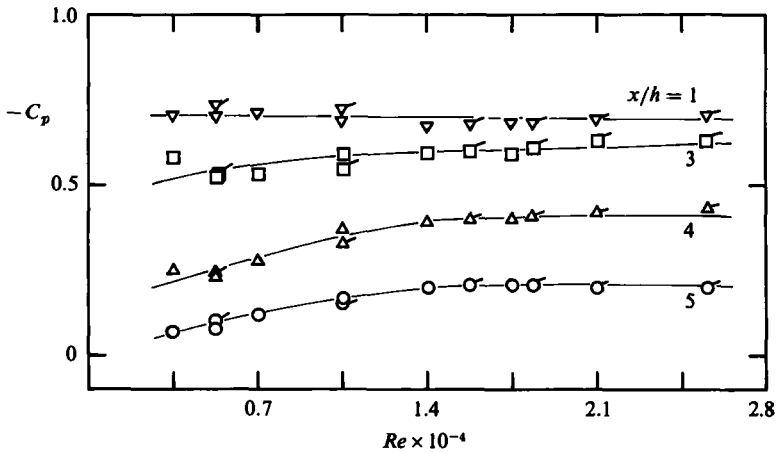


FIGURE 3. Reynolds-number dependence of the pressure coefficients. Plain symbols, $h = 1$ cm; dashed symbols, 1.5 cm.

speed for vortex shedding. The velocity fluctuation was measured using a constant-temperature hot-wire anemometer. The hot wire was $6h$ downstream of the leading edge and $1.5h$ above the top surface.

3. Experimental results and discussions

The measurements were concerned with flat-plate models of different thicknesses, mounted in a closed working section, and exposed to smooth and turbulent flows of a constant speed. Apart from turbulence, there are many factors that can affect the flow past the model. These include, among others, the ratios of chord and span to thickness, the Reynolds number and the tunnel blockage.

The pressure distribution along the separation bubble (see figure 4) is characterized

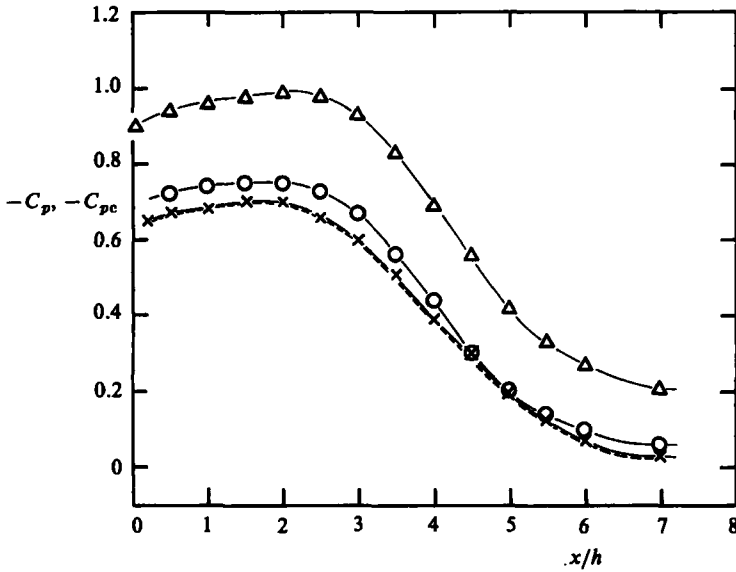


FIGURE 4. Pressure distributions on models with $h = 1, 6$ and 20 cm in smooth flow. \times , $h = 1$ cm; O , 6 cm; Δ , 20 cm; ----, corrected for blockage.

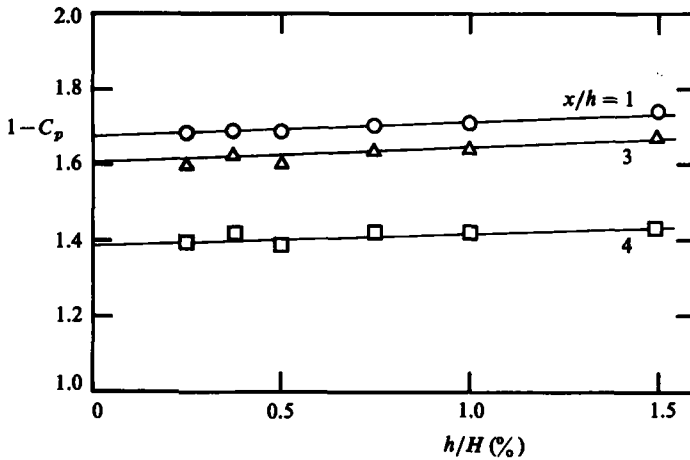


FIGURE 5. Blockage effect in smooth flow.

by a low-pressure plateau near the separation point followed by a rapid recovery towards the reattachment point. The minimum value of chord-to-thickness ratio for the model was about 17. This is regarded as large enough for vortex shedding at the trailing edge not to affect the bubble flow near the leading edge.

3.1. Spanwise pressure distributions

The minimum value of span-to-thickness ratio for the model was about 28. This is also regarded as large enough. Figure 2 shows some examples of the spanwise pressure distributions for smooth and turbulent flows. As can be seen, the pressure along the span is reasonably uniform for both smooth and turbulent flows.

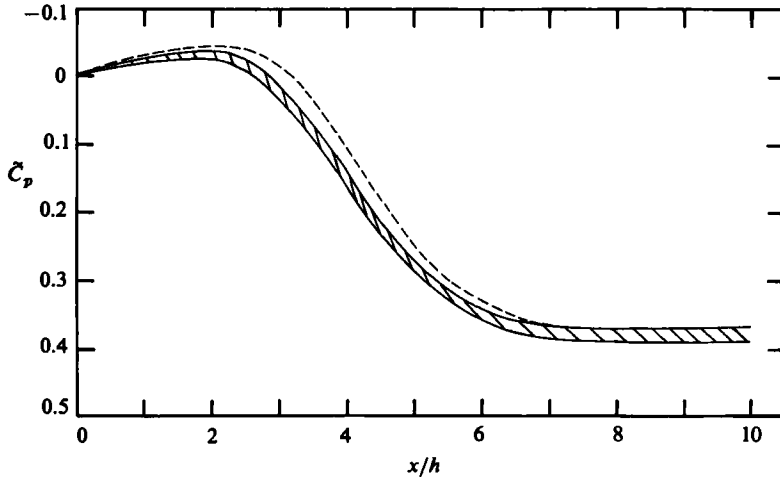


FIGURE 6. Reduced pressure distributions in smooth flow. All measurements corresponding to six different values of h fall within hatched area. ----, $h = 20$ cm.

3.2. Reynolds-number effects

Figure 3 shows the effects of Reynolds number on the pressure coefficients for smooth flow at four selected positions using models with $h = 1$ and 1.5 cm. The results indicate that the pressure coefficients for smooth flow are reasonably independent of the Reynolds number if it is approximately greater than 1.4×10^4 , a value equivalent to a combination of $h = 1$ cm and $U = 20$ m s⁻¹. We can assume that if there is no Reynolds-number effect for smooth flow, there would be also no such effect for turbulent flow (Nakamura & Ohya 1984). On this basis a flow speed of 20 m s⁻¹ was employed for models with $h = 1$ and 1.5 cm, and of 10 m s⁻¹ for the other models, mainly for time economy.

3.3. Blockage effects

Figure 4 shows measured (uncorrected) pressure distributions on models with $h = 1$ and 6 cm in smooth flow, and all the pressure distributions for other values of h are found to fall in between these two. Figure 4 also shows the pressure distribution for the model with $h = 20$ cm which was used for the oscillating-spoiler experiment. The difference in pressure distribution among models is obviously due to tunnel blockage. In figure 5 pressure coefficients at several representative points are plotted in the form of $1 - C_p$ against the blockage ratio h/H , where H is the tunnel height. The results suggest that the pressure coefficient for small values of h/H can be written using a constant correction factor ξ as

$$1 - C_p = (1 - C_{pc}) \left(1 + \xi \frac{h}{H} \right), \quad (1)$$

where C_{pc} is the corrected pressure coefficient. In other words, the pressure distributions in the confined flow are similar in shape, in agreement with the basic assumption of Maskell's (1965) theory of blockage correction. The corrected pressure distribution is also shown in figure 4. In the present experiment it was assumed that (1) with the same correction factor could be applied to measurements in turbulent flow.

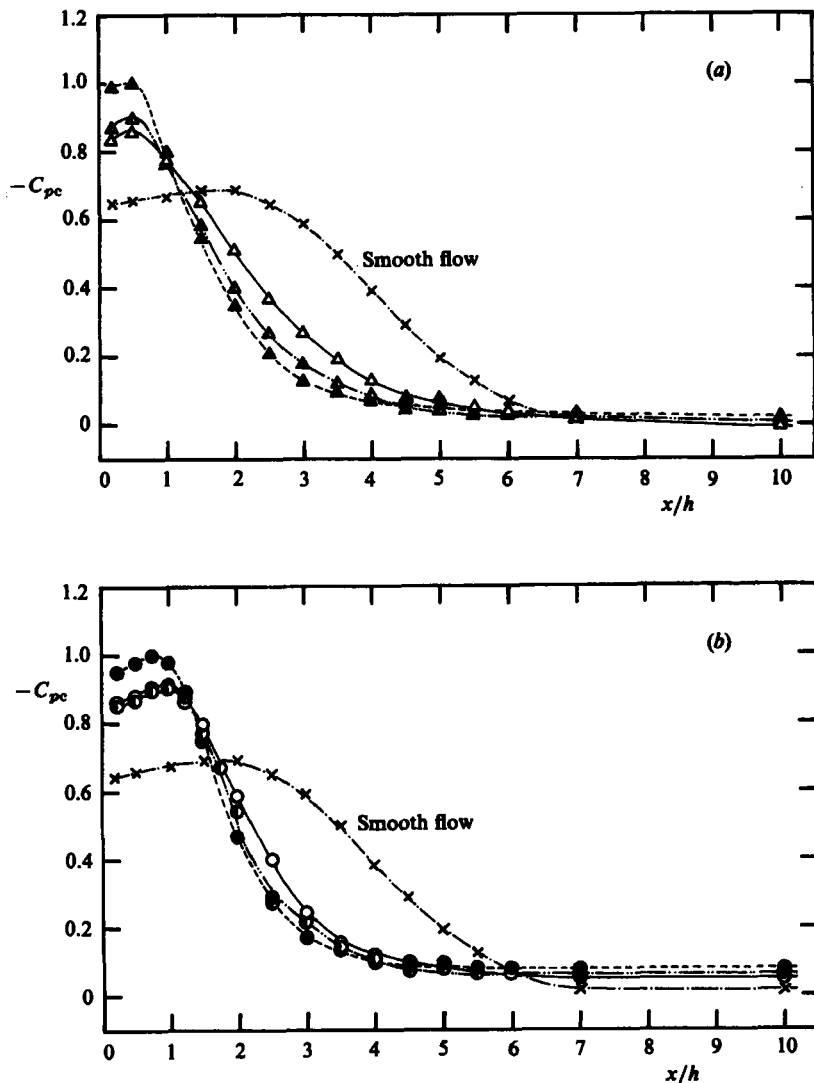


FIGURE 7. Corrected pressure distributions in smooth and turbulent flows. (a) $h = 1$ cm. \blacktriangle , $L_x/h = 3.0$, $u'/U = 12.8\%$; \triangle , 8.4, 11.2%; \blacktriangle , 16.5, 11.0%; (b) $h = 6$ cm. \bullet , $L_x/h = 0.65$, $u'/U = 6.9\%$; \circ , 2.1, 7.3%; \bullet , 4.0, 6.6%.

Observation of similarity in pressure-distribution shape in the bubble region for various separated and reattaching flows has led to various attempts to produce a more universal correlation of mean pressure data (Norbury & Crabtree 1955; Roshko & Lau 1965). Following Roshko & Lau, we define the reduced pressure coefficient as

$$\bar{C}_p = \frac{C_p - C_{ps}}{1 - C_{ps}}, \quad (2)$$

where C_p and C_{ps} are the uncorrected pressure coefficients with the suffix s representing the separation point. In the present experiment C_{ps} was determined from extrapolation of the pressure distribution. The reduced pressure coefficient \bar{C}_p

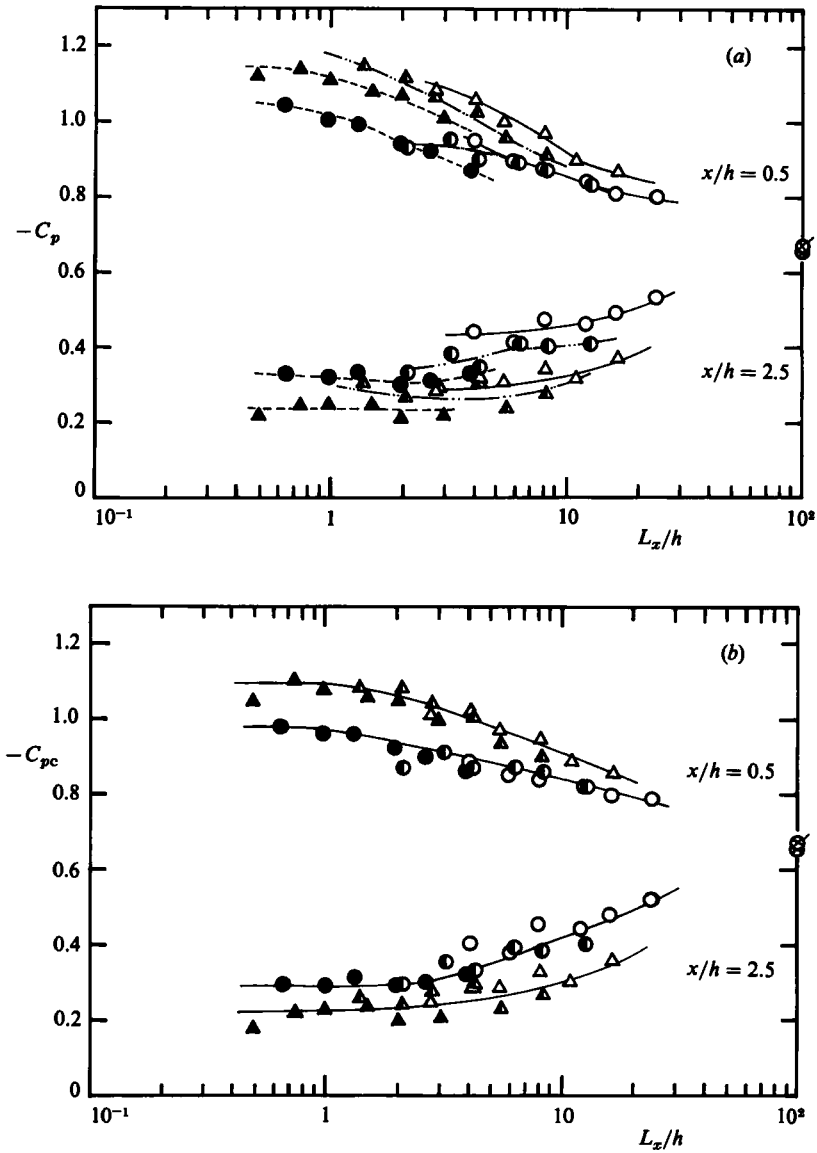


FIGURE 8. Variation of the pressure coefficients at $x/h = 0.5$ and 2.5 with turbulence scale for high and low intensities of turbulence. (a) Uncorrected for blockage. (b) Corrected for blockage. Grid: A, ▲; B, △; C, △ (all with high u'/U). Grid: A, ●; B, ○; C, ○ (all with low u'/U). ⊗, Smooth flow, $x/h = 0.5$; ⊗, smooth flow, 2.5 .

is expected to be free from tunnel blockage if Maskell's assumption mentioned above is correct. This is shown in figure 6 in which all the pressure distributions corresponding to six different values of h collapse roughly onto a single curve. The broken line in the figure also shows the reduced pressure distribution corresponding to $h = 20$ cm. The results of measurements in turbulent flow in the following sections are presented in terms of either the corrected pressure coefficient C_{pc} or the reduced pressure coefficient \bar{C}_p .

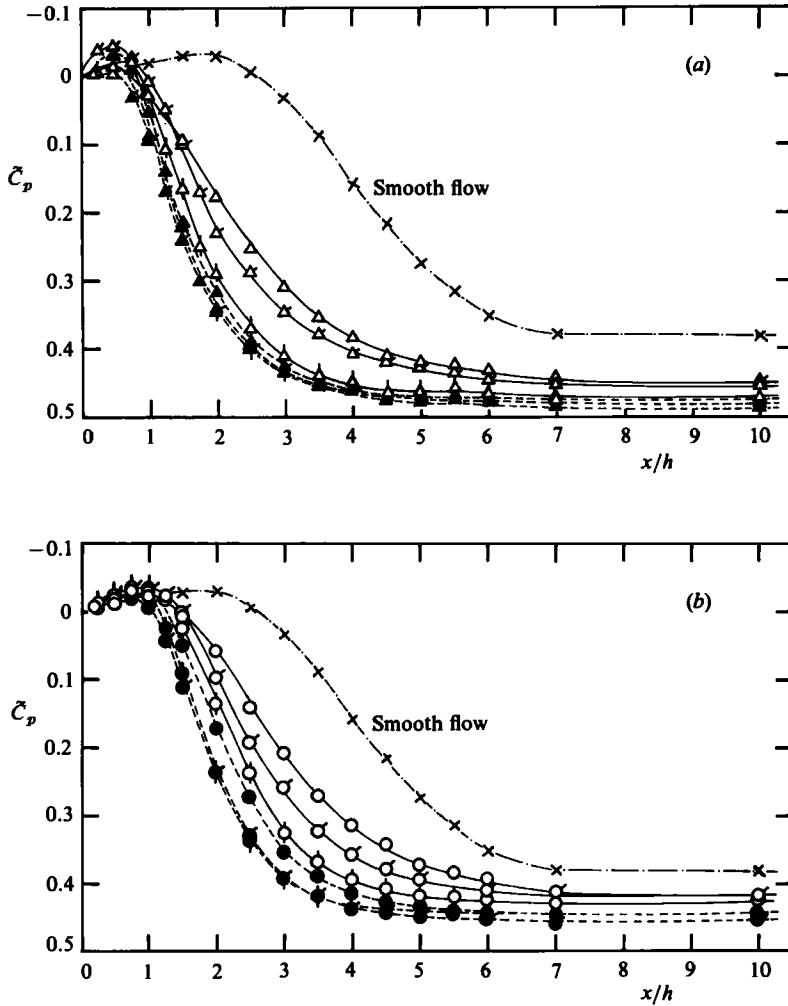


FIGURE 9. Reduced pressure distributions in smooth and turbulent flows for high and low intensities of turbulence. (a) Grid A: $L_x/h = \blacktriangle, \circ, 5; \blacktriangle, 1.5; \blacktriangle, 3.0$. Grid C: $L_x/h = \triangle, 2.8; \triangle, 8.3; \triangle, 16.5$ (high u'/U for all readings). (b) Grid A: $L_x/h = \bullet, 0.7; \bullet, 2.0; \bullet, 3.9$. Grid C: $L_x/h = \circ, 4.0; \circ, 12.0; \circ, 24.0$ (low u'/U for all readings).

3.4. The effects of turbulence scale

Figure 7(a) shows the corrected pressure distributions on the model with $h = 1$ cm in smooth and turbulent flows, while figure 7(b) shows similar results on the model with $h = 6$ cm. In agreement with previous measurements, the results indicate that the main effect of free-stream turbulence is to produce a considerable contraction of the bubble length.

Figure 8(a) shows uncorrected pressure coefficients at two representative positions of $x/h = 0.5$ and 2.5 plotted against turbulence scale L_x/h for two values of turbulence intensity. Although the pressure coefficients shown in figure 8(a) are apparently changing with turbulence scale, we should avoid drawing any definite conclusions unless the blockage effects are correctly eliminated. The variations of the corrected pressure coefficients with turbulence scale are shown in figure 8(b). As can be seen,

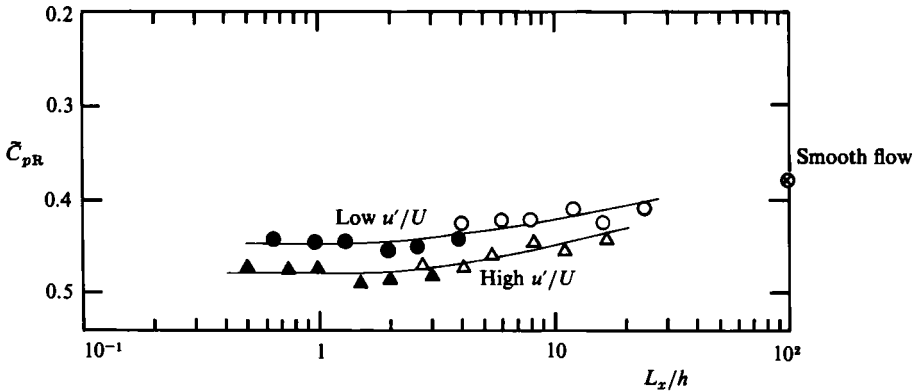


FIGURE 10. Variation of the reduced reattachment pressure with turbulence scale.
 ●, ▲, grid A; ○, △, grid C.

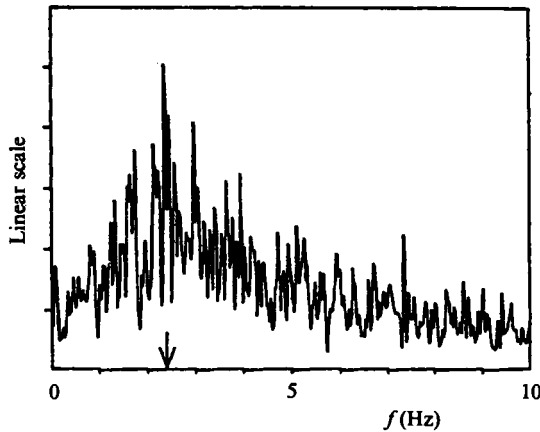


FIGURE 11. Power spectrum of the u -component velocity fluctuation for the model with $h = 20$ cm without spoiler oscillation. The measurements were made at $x = 6h$ and $1.5h$ above the plate surface at $U = 4 \text{ m s}^{-1}$.

overlapping of data on models with different thicknesses using different turbulence-producing grids is reasonably satisfactory. This confirms the validity of the blockage correction used in the present paper.

Figure 8(b) shows that the pressure coefficients are almost insensitive to changing turbulence scale up to approximately $L_x/h = 2.0$. This is in agreement with Hillier & Cherry (1981). With further increase in turbulence scale, however, the pressure coefficients are asymptoting towards corresponding smooth-flow values. It is suggested that turbulence of very large scale is equivalent to a flow with slowly fluctuating velocity, and hence it can no longer influence the bluff-body mean flow effectively. The effect of turbulence scale is more directly seen in the reduced pressure distributions shown in figure 9(a, b), where the results on models with $h = 1, 2$ and 6 cm using two turbulence-producing grids (grids A and C) are plotted. The experiment for small-scale turbulence using grid A indicates that the pressure distribution is almost insensitive to changing turbulence scale. By contrast, the experiment for large-scale turbulence using grid C indicates that the pressure distribution is asymptoting towards that for a smooth-flow with increasing turbulence scale.

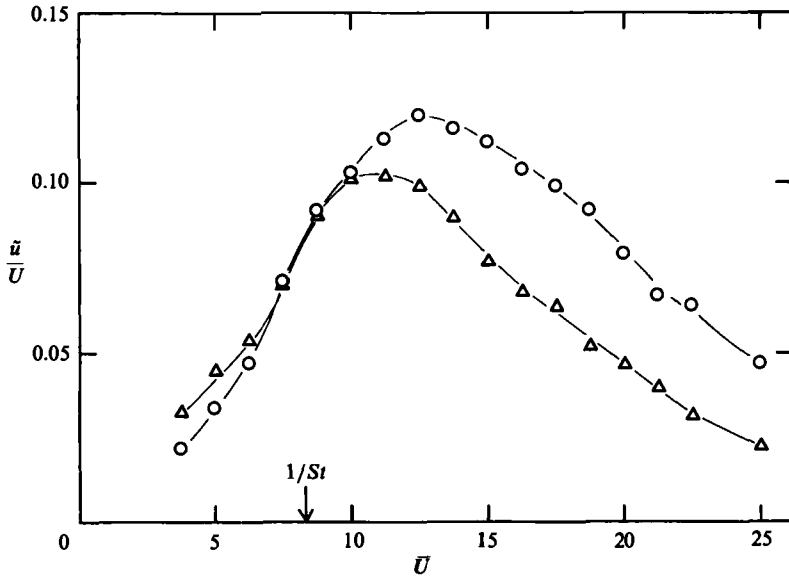


FIGURE 12. Velocity fluctuations for the model with spoiler oscillation at amplitudes of $0.05h$ and $0.1h$. Δ , $0.05h$; \circ , $0.1h$. The arrow indicates the resonance speed for vortex shedding. The position of measurement is the same as in figure 11.

Figure 10 shows the variations of the reduced reattachment pressure \bar{C}_{pR} with turbulence scale, where \bar{C}_{pR} is defined as the reduced pressure coefficient for the maximum value of pressure distribution data such as shown in figure 9. The results indicate that \bar{C}_{pR} is changing with both the intensity and scale of turbulence, and it is again asymptoting towards the smooth-flow value as the turbulence scale increases beyond approximately $L_x/h = 2.0$.

3.5. The experiment with an oscillating leading-edge spoiler

Observations by Cherry, Hillier & Latour (1983, 1984) and Kiya & Sasaki (1984) showed that the separated and reattaching flow is not always steady but includes vortex shedding of weak periodicity. Nakamura & Nakashima (1986) recently suggested that it is a form of the impinging-shear-layer instability. The purpose of the experiment in this section is to see how oscillation of a leading-edge spoiler affects the mean pressure field on a flat plate through its influence on vortex shedding.

Figure 11 shows the power spectrum of the u -component velocity fluctuation measured at $x = 6h$ and $1.5h$ above the top surface of a flat-plate model when the leading-edge spoiler is not oscillating. It can be seen that there is a weak periodicity in the spectrum in agreement with Cherry *et al.* (1983); the value of the Strouhal number St based on h is found to be approximately 0.12.

Figure 12 shows how velocity fluctuation responds to the spoiler oscillation. The results are presented for two values of oscillation amplitude: $0.05h$ and $0.1h$. The position of the hot wire was the same as in figure 11. \tilde{u} represents the component of the velocity fluctuation which has the same frequency as that of the spoiler oscillation, and was obtained with a real-time FFT analyser. As can be seen, there is a mild peak in \tilde{u}/U and, as the amplitude of spoiler oscillation is lowered, the reduced speed at which the peak occurs approaches the resonance speed which is equal to the inverse of the Strouhal number and shown by an arrow in the figure. Clearly, this indicates a weak resonance of vortex shedding due to the spoiler oscillation.

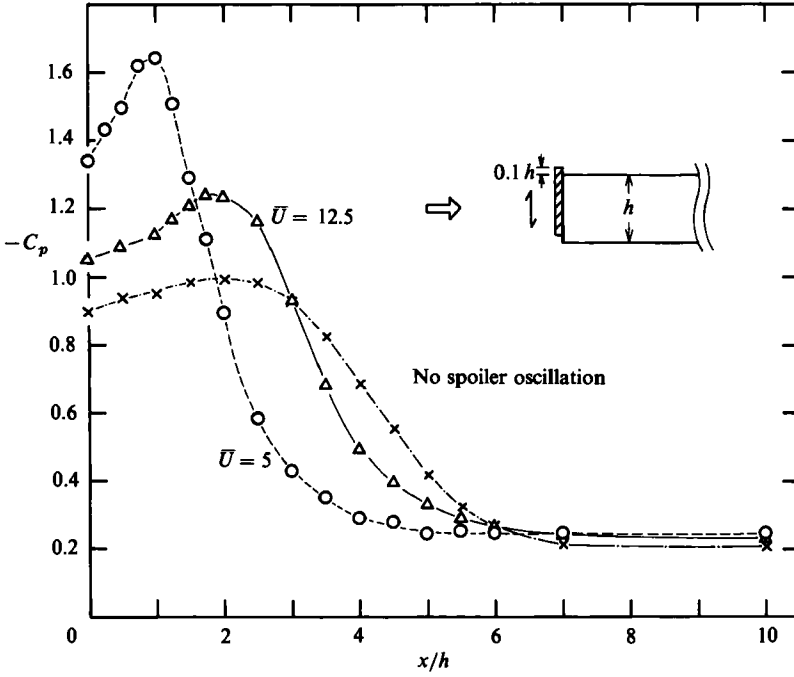


FIGURE 13. Pressure distributions for the model with and without spoiler oscillation at an amplitude of $0.1h$.

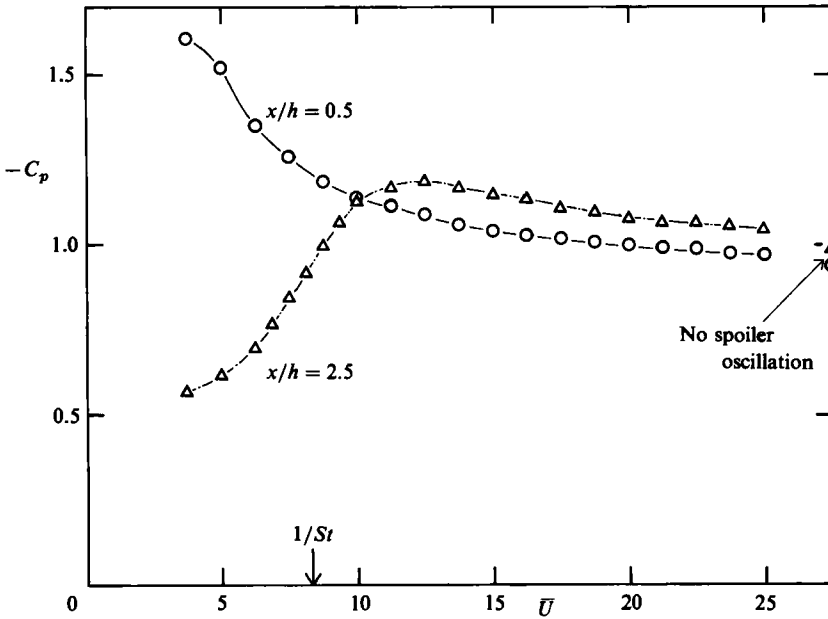


FIGURE 14. Pressure coefficients at $x/h = 0.5$ and 2.5 for the model with spoiler oscillation at an amplitude of $0.1h$. The arrow indicates the resonance speed for vortex shedding.

Figure 13 shows three representative pressure distributions along the separation bubble for the model with and without spoiler oscillation at an amplitude of $0.1h$. Figure 14 shows the variation of the pressure coefficients at $x/h = 0.5$ and 2.5 with the reduced speed. The pressure coefficients presented are uncorrected for tunnel blockage. Figure 13 shows that the main effect of the spoiler oscillation is to shorten the separation bubble: it is shortened progressively with decreasing reduced speed. Figure 14 shows that the value of $-C_p$ at $x/h = 0.5$ increases progressively with decreasing reduced speed while that at $x/h = 2.5$ has a peak at about $\bar{U} = 11.0$. Although the reduced speed for the peak is close to the resonance speed, the peak is not associated with vortex resonance. Any point between the separation point and that corresponding to the minimum pressure on the separation bubble in smooth flow (figure 13) can have such a peak, and the reduced speed at which the peak occurs is lowered as the point is closer to the separation point. In summary, the results indicate no significant trace of vortex resonance in the mean pressure distribution. This may be because vortex resonance is weak enough not to affect the mean pressure field significantly.

4. The interaction between large-scale turbulence and the impinging-shear-layer instability

As was shown earlier (Nakamura & Ohya 1984), one of the main effects of large-scale turbulence is to interact with the Kármán vortex trail from a two-dimensional bluff body to weaken it by reducing spanwise correlation. In the present study we are concerned with the interaction between large-scale turbulence and the impinging-shear-layer instability, of which little has been known to date.

We have shown that the mean pressure field along the separation bubble asymptotes towards the smooth-flow field if the turbulence scale is increased beyond approximately $L_x/h = 2.0$, but there is no significant trace of an interaction between large-scale turbulence and the impinging-shear-layer instability (figure 8*b*). It is suggested that the interaction would be weak enough not to affect the mean pressure field significantly. This view is supported by the oscillating-spoiler experiment in smooth flow which shows that vortex resonance due to two-dimensional disturbance is weak enough not to affect the mean pressure field significantly.

5. Conclusions

The effect of free-stream turbulence on the mean pressure distribution along the separation bubble formed on a flat plate with rectangular leading-edge geometry has been investigated experimentally in a wind tunnel using turbulence-producing grids. The ratio of turbulence scale to plate thickness investigated ranges from about 0.5 to 24 for two values of turbulence intensity of about 7 and 11 %, and emphasis is placed on finding the effect of turbulence scale.

It is found that the main effect of free-stream turbulence is to shorten the separation bubble. It is shortened progressively with increasing turbulence intensity. The mean pressure distribution along the shortened separation bubble is insensitive to changing turbulence scale up to a scale ratio of about two. This result for small-scale turbulence is in agreement with Hillier & Cherry (1981). With further increase in the scale ratio, however, the mean pressure distribution asymptotes towards the smooth-flow distribution. This means that turbulence of very large scale is equivalent to a

flow with slowly fluctuating velocity so that it can no longer influence the mean flow effectively. There is no trace of an interaction between large-scale turbulence and vortex shedding (impinging-shear-layer instability) in the mean pressure distribution. Probably, the interaction would be weak enough not to affect the mean pressure field significantly. This view on the interaction between large-scale turbulence and vortex shedding is supported by an oscillating leading-edge spoiler experiment in smooth flow which shows that although there is a weak resonance with vortex shedding due to the spoiler oscillation, there is no trace of vortex resonance in the mean pressure field.

We thank Messrs N. Fukamachi, K. Watanabe and T. Shoji for their help in conducting the experiment. This work was supported in part by a grant from the Ministry of Education, Science and Culture of Japan.

REFERENCES

- BEARMAN, P. W. 1978 In *Proc. 3rd US Natl Conf. Wind Engng Res., Univ. Florida* (ed. B. M. Leadon), pp. 265-272. University of Florida.
- BEARMAN, P. W. & MOREL, T. 1983 *Prog. Aero. Sci.* **20**, 97-123.
- CHERRY, N. J., HILLIER, R. & LATOUR, M. E. M. P. 1983 *J. Wind Engng Indust. Aero.* **11**, 95-105.
- CHERRY, N. J., HILLIER, R. & LATOUR, M. E. M. P. 1984 *J. Fluid Mech.* **144**, 13-46.
- HILLIER, R. 1976 *CERL Rep.* RD/L/N242/75.
- HILLIER, R. & CHERRY, N. J. 1981 *J. Wind Engng Indust. Aero.* **8**, 49-58.
- KIYA, M. & SASAKI, K. 1984 *Bull. Japan Soc. Mech. Engrs* **50**, 1483-1490 (in Japanese).
- KIYA, M., SASAKI, K. & ARIE, M. 1984 *Bull. Japan Soc. Mech. Engrs* **50**, 967-973 (in Japanese).
- MASKELL, E. C. 1965 *Aero. Res. Counc. R & M* 3400.
- NAKAMURA, Y. & NAKASHIMA, M. 1986 *J. Fluid Mech.* **163**, 149-169.
- NAKAMURA, Y. & OHYA, Y. 1983 *J. Fluid Mech.* **137**, 331-345.
- NAKAMURA, Y. & OHYA, Y. 1984 *J. Fluid Mech.* **149**, 255-273.
- NAKAMURA, Y. & OHYA, Y. 1986 *J. Fluid Mech.* **164**, 77-89.
- NOBURY, J. F. & CRABTREE, L. F. 1955 *RAE Tech. Note Aero* 2352.
- ROSHKO, A. & LAU, J. K. 1965 In *Proc. 1965 Heat Transfer and Fluid Mech. Inst.* (ed. A. F. Charwat), pp. 157-167. Stanford University Press.